



HAL
open science

Acoustic system for average temperature measurement in an industrial environment

Karim Mimoune, Joffray Guillory, Cécile Guianvarc'H, Mark Plimmer

► **To cite this version:**

Karim Mimoune, Joffray Guillory, Cécile Guianvarc'H, Mark Plimmer. Acoustic system for average temperature measurement in an industrial environment. Forum Acusticum, Dec 2020, Lyon, France. pp.3373-3379, 10.48465/fa.2020.0941 . hal-03233973

HAL Id: hal-03233973

<https://hal.science/hal-03233973>

Submitted on 13 Jun 2021

HAL is a multi-disciplinary open access archive for the deposit and dissemination of scientific research documents, whether they are published or not. The documents may come from teaching and research institutions in France or abroad, or from public or private research centers.

L'archive ouverte pluridisciplinaire **HAL**, est destinée au dépôt et à la diffusion de documents scientifiques de niveau recherche, publiés ou non, émanant des établissements d'enseignement et de recherche français ou étrangers, des laboratoires publics ou privés.

Acoustic system for average temperature measurement in an industrial environment

Karim MIMOUNE¹

Joffray Guillory¹

Cécile Guianvarc'h¹

Mark Plimmer¹

¹ Laboratoire Commun de Métrologie (LCM), CNAM, France
Karim-mounssif.mimoune@lecnam.net

ABSTRACT

The accuracy of length measurements performed in harsh industrial environments by optical systems, such as laser trackers and absolute distance meters, for the dimensional inspection of large mechanical parts, strongly depends on the air refractive index. The latter is usually calculated as a function of ambient conditions i.e. temperature, pressure, humidity and CO₂ content using the Edlen formula. Its value should be carefully controlled during length measurements. In industrial environments, monitoring all these parameters, especially temperature, with sufficient accuracy can be most difficult. Indeed, the industrial workspaces can be subjected to temperature gradients of few degrees, and an uncertainty of 1°C in the temperature estimation leads to an uncertainty of 1 μm/m in distances measured optically.

The aim of this work is to develop and optimize an acoustic thermometer able to perform real-time measurements of the average air temperature along an optical pathway. This apparatus is destined to be integrated into a laser absolute distance meter to improve its performances. The acoustic thermometer presented in this paper is based on the measurement of the time of flight of acoustic pulses between two measuring heads. The requirements for such a thermometer, for measurements in industrial environments, make the technical choices and practical realization challenging. Indeed, the working frequency range should be in the ultrasonic region, which implies a strong attenuation of the acoustic waves in air and correspondingly a low signal-to-noise ratio. Moreover, the whole measurement system should remain compact, with wireless communication between the measuring heads.

1. INTRODUCTION

In many high value industries, such as car manufacturing and aerospace, the dimensional requirements on large mechanical parts are becoming ever more stringent. On the one hand, this stimulates the improvement of machine tools, especially their positioning. On the other hand, it leads to the development of dimensional inspection systems able to check the conformity to the intended design. This evolution is assisted by large volume

metrology, a field in which the ability to provide high accuracy coordinate systems is essential.

Most of these positioning systems are based on optical measurements and their accuracy depends in part on the knowledge of the air refractive index n_{air} . Indeed, a mechanical distance measured by an optical interferometric system (such as laser trackers) or a system based on phase measurements of an RF modulated optical wavelength relies on the knowledge of the speed of light in the air, which depends on the temperature, pressure, humidity and CO₂ content. Therefore, the measured distances must be corrected by the air refractive index using an updated version of Edlen's formula [1]. In this formula, the temperature is the largest contributing factor, an error of 1 °C over the optical path inducing an error of 1 μm per meter in the distance measurement.

For systems based on angle measurements, such as photogrammetry or laser trackers, it is assumed that light travels in straight lines. However, in harsh environments where (mainly vertical) temperature gradients can occur, optical refraction causes bending of the measurement path. Such cases are considered in [2], [3] where beam deflections of up to several tens of micrometers are reported.

Among the positioning systems, laser trackers, based on a distance measurement with two angle measurements, are subject to both effects and require corrections derived from the average temperature and the temperature gradient between the instrument and the target.

To avoid this dual effect, we are developing a multilateration coordinate system based on distance measurements only [4]. To determine the average temperature, this system will be equipped with acoustic thermometers able to measure the effective air temperature along each optical path. For this purpose, the high sensitivity of the speed of sound to air temperature is exploited.

In the remainder of this paper, the relation between speed of sound and temperature is explained (section 2), after which the acoustic thermometer is presented (section 3). In section 4, the procedure for temperature measurement is detailed, from signal generation to signal processing, as well as calibration. Lastly, in section 5, a few experimental results are presented and discussed.

2. ACOUSTIC THERMOMETER PRINCIPLE

The acoustic thermometer presented in this paper is based on the measurement of the time of flight (TOF) τ of an acoustic wave travelling in the air from a transmitter to a receiver separated by a known distance d . The speed of sound in the air u is then directly given by

$$u = d/\tau \quad (1)$$

Its value depends on the temperature, and to a lesser extent on the static pressure, humidity and CO₂ content. Under the assumption of static pressure, humidity and CO₂ content spread equally across the room, a system equipped with local sensors is able to determine the average temperature along the path of the acoustic wave from TOF measurements.

The speed of sound u in a non-ideal gas can be written as a classical virial expansion as follows

$$u^2 = \gamma RT/M (1 + 2PB/RT) \quad (2)$$

where R is the universal gas constant, γ the specific heat ratio, T the thermodynamic temperature, M the molecular mass, P the static pressure and B the second virial coefficient of air [5].

In practice, formula (2) is difficult to apply because the parameters γ , M and B are not measured directly but derived from humidity and CO₂ measurements. For such applications, therefore, the use of empirical Cramer [5] and Wong [6] equations is more convenient since they describe the speed of sound directly as a function of temperature, static pressure, water vapor mole fraction x_w and CO₂ mole fraction x_c as follows

$$u = a_0 + a_1\theta + a_2\theta^2 + (a_3 + a_4\theta + a_5\theta^2)x_w + (a_6 + a_7\theta + a_8\theta^2)P + (a_9 + a_{10}\theta + a_{11}\theta^2)x_c + a_{12}x_w^2 + a_{13}P^2 + a_{14}x_c^2 + a_{15}x_wPx_c \quad (3)$$

where θ is the air temperature expressed in degree Celsius and the a_i are empirically determined coefficients [5], [7] The validity of this equation has been verified for the temperatures from 0 °C to 30 °C, static pressures from 750 hPa to 1020 hPa, up to 0.06 water mole fraction and up to 1% of CO₂ concentration, which cover the environmental conditions for the acoustic thermometer developed here. Uncertainties in the values of the speed of sound using this equation have been estimated to about 300 ppm.

3. ACOUSTIC THERMOMETRIC SYSTEM

3.1 Technical description and operation mode

The acoustic thermometer we are developing is designed to estimate the average temperature along distances up to 20 m. Fig.1-a and Fig.1-b show, respectively, top and fronts view of the apparatus. It is composed of two pairs of ultrasonic transducers, one used as a transmitter, the other as a receiver (from T1 to R1 and from T2 to R2),

each pair of transducers being used for TOF measurements along a path. To compensate possible airflow effects (*cf.* § 3.2), TOF measurements along the two paths are performed in both directions. The system also requires a distance measurement of the path, which is performed by a commercial laser distance meter (Leica Disto D210).

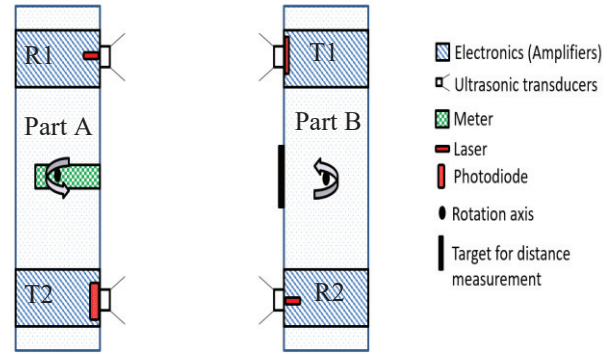


Figure 1-a. Global architecture of the acoustic thermometer (top view).

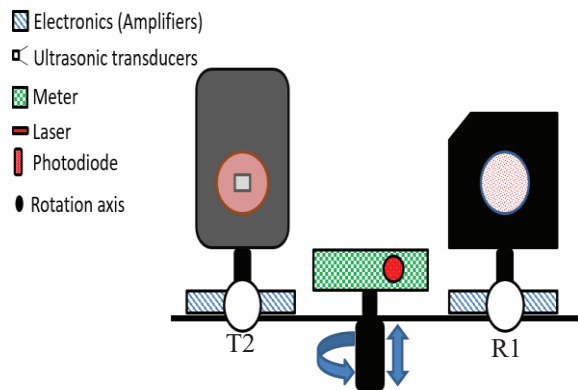


Figure 1-b. Architecture of part A (R1 and T2) of the acoustic thermometer (front view) shown above in Fig. 1a.

The software controlling the whole system and performing real-time signal processing and data analysis is Matlab®. For a given path, depicted in Fig. 2, a harmonic pulse signal is first digitally synthesized and sent by Wi-Fi to a signal generator and acquisition card (STEMlab 125-14 Red Pitaya board) for emission of the signal. At this point, the signal passes through a 90/10 RF splitter (Mini-Circuits ZFDC-10-6-s+): 90% of the power is sent back to the Red Pitaya to be used as a reference for the TOF measurement, while 10 % of the power modulate a fibre-optic laser (Thorlabs LPS-635-FC) mounted on a kinematic mirror mount (Thorlabs KM100T). The signal is thus transferred optically (wireless solution) to the transmission part of the system where an amplified photodiode receives the signal (Thorlabs PDA36A-EC). This signal is then electronically amplified, sent to the acoustic transducer T2 (Cebek C7210) and transmitted acoustically back towards the receiving transducer R1 (Massa TR-89B).

The received signal is then amplified and sent to the Red Pitaya to be used as a measured signal for the TOF measurement. Both the reference and the measured signal are stored. A microcontroller is also attached to the Red Pitaya board for

- controlling the gain of the electronic amplifier at the receiver to avoid saturation of the received signal,
- recording data from pressure and humidity sensors (CO₂ concentration is set arbitrarily to 400 ppm).

Once all the data have been acquired by the Red Pitaya board, they are sent back to the computer for processing.

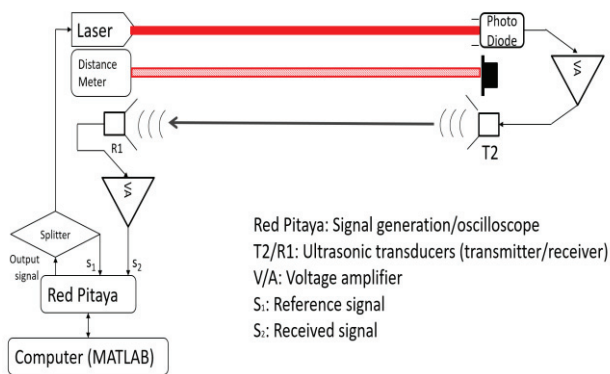


Figure 2. Principle of the TOF measurement

3.2 Airflow effect compensation

During the TOF measurement of an acoustic wave, the presence of an airflow along the propagation axis can directly impact the results by increasing or decreasing the measured speed of sound, depending on the airflow direction with respect to those of the acoustic propagations. This induces errors in the speed of sound measurements, and hence in the resulting mean temperature calculations.

To cancel these, two symmetrical paths between acoustic transmitter and receiver have been set up: since the measurements on both paths cannot be made simultaneously, they are carried out within 2.5 s of each other (shortest achievable interval for the acquisitions) during which time the airflow is assumed to remain constant to the required level. At the end, the value of the speed of sound u retained here is the average value between the measured speeds u_1 (direction A to B) and u_2 (direction B to A) as depicted in Fig. 3.

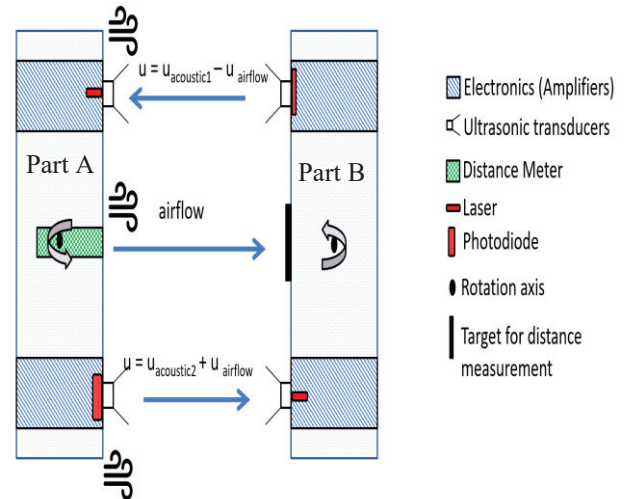


Figure 3. Airflow effect compensation with bidirectional speed of sound measurement.

4. EXPERIMENTAL PROCEDURE

The system has been developed with low cost in mind. The use of relatively cheap transducers and electronic components can lower the signal-to-noise ratio of the received signal compared with expensive ones. Under these hardware constraints, we seek to optimize the acoustic pulse signal, i.e. its waveform and frequency range, and the signal processing techniques in order to reduce the measurement uncertainties as well as maximize the distance range covered by the thermometer.

4.1 Acoustic transmission

For the sake of industrial on-site applications, user comfort requires one work in an inaudible frequency range. We selected piezoelectric transducers operating at low ultrasonic frequencies, around 40 kHz, in order to maintain an acceptable sound attenuation in air (about 1.3 dB/m at 40 kHz). Such kind of transducers are also directional, which matches with the present requirements of increasing the acoustic power transmitted to the receiving transducer while limiting as much as possible the ultrasonic power possibly transmitted to users (safety concerns)[8]. Moreover, these ultrasonic transducers are compact and widely commercially available.

To increase the operating distance range, the transmitter is equipped with an operational amplifier with a fixed voltage gain to maximize the emitted signal power with the highest possible SNR. The receiving transducer is equipped with an operational amplifier as well, with variable gain with the purpose of amplifying and adapting the incoming signal to the analog/digital converter of the Red Pitaya board. The amplifiers are designed to be effective at the working frequencies of the transducers. Figure 4 shows the frequency response of the system

from 36 kHz to 44 kHz, measured with the transducers and amplifiers separated by 10 m and emitting a continuous sinusoidal signal.

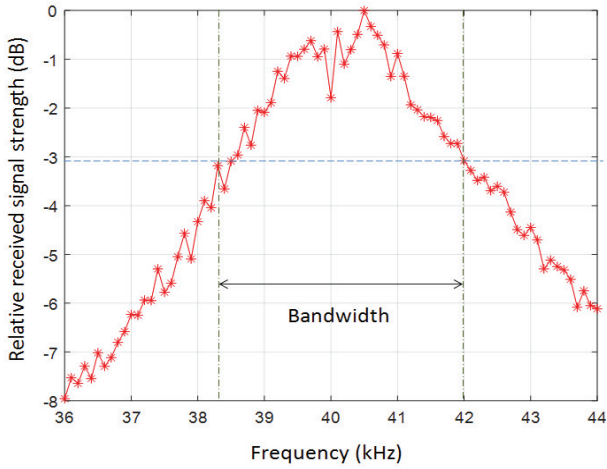


Figure 4. Relative received signal strength as a function of the frequency and the bandwidth at -3 dB.

4.2 Signal Processing

The spectral content of the generated signal should remain in the bandwidth of the system shown in Fig. 4, which constrains the frequency range of the generated pulses.

In practice, a linear frequency modulation (linear chirp) from 38 kHz to 42 kHz has been chosen for the harmonic pulse signal in order to benefit of the pulse-compression techniques. For reasons of low SNR on the received signal in our measurement conditions, threshold detection techniques are not considered here. Techniques relying on the analysis of the generated and received signals such as cross-correlation provide more efficient noise reduction [9]. Indeed, the autocorrelation function of a linear chirp pulse of duration T , central instantaneous frequency f_0 and bandwidth Δf has approximately the following shape:

$$f(t) = \text{tri}(t/T) \times \text{sinc}[\pi \Delta f t \text{tri}(t/T)] \times \sin(2\pi f_0 t) \quad (4)$$

where $\text{tri}(t/T)$ denotes the triangle function. By choosing a bandwidth satisfying the criterion $T\Delta f > 1$ allows one to narrow the main lobe of the autocorrelation function and thus increase the resolution of the detection process. In practice, T needs to be short enough to avoid overlapping echoes that could possibly deteriorate the received signal, so the time bandwidth product is set to 2. ($T=500 \mu\text{s}$)

Actually, while the maximum of a direct detection of the cross-correlation function gives good results, other techniques listed in [10], [11] are still under consideration, provided they comply with the requirements of real-time processing. Fig. 5-a shows the

reference signal (in blue) and the received signal (in red) while Fig. 5-b depicts the cross-correlation result of these two signals

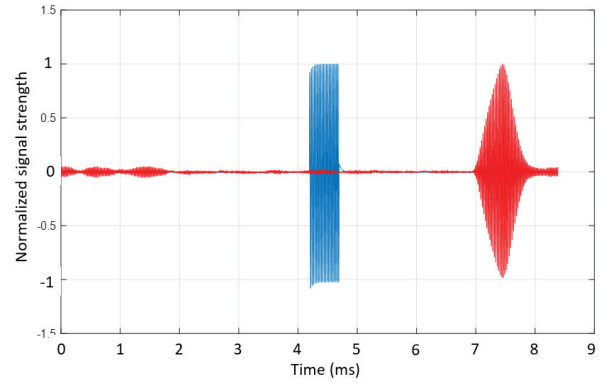


Figure 5-a. Normalized reference acoustic signal (blue, center) and normalized received signal (red)

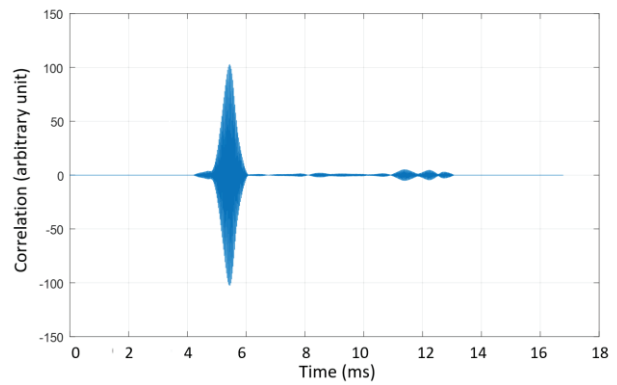


Figure 5-b. Cross-correlation of the reference and received signals.

4.3 System calibration

Basically, the time difference between the received signals is not exactly the TOF of the acoustic wave. Indeed, this time difference of arrival (TDOA) t_d includes an offset t_{off} due to the electronic components and cables, which is intrinsic to the system and assumed to be constant. To determine it, the system has to be calibrated for each direction, this offset can be calculated using equation (5):

$$u = d / \tau = d / (t_d - t_{off}) \quad (5)$$

The calibration process consists in performing TDOA measurements for different distances, from 3.3 m to 11.8 m, at a stable temperature known thanks to the setting up of six temperature sensors (100 Ω platinum resistance thermometers Pt100) separated by 2 m along a 10 m path. In parallel, the theoretical TOF of the acoustic wave is calculated from the distance meter of the system for d and from Cramer's formula and the reference temperatures (Pt100) for u . In this way, the theoretical TOF can be compared to the TDOA measured by the system: the value of the offsets has been estimated for

each distance of the calibration process (Table II). An example of the application of these offsets on temperature measurements is provided in Fig. 6-a for a distance of 10.309 m, as well as the temperature difference (labelled “error”) in Fig. 6-b.

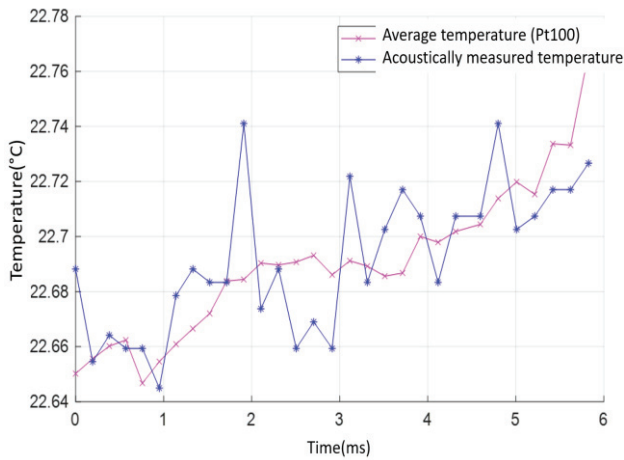


Figure 6-a. Temperature measurements over 10.309 m with an optimal offset.

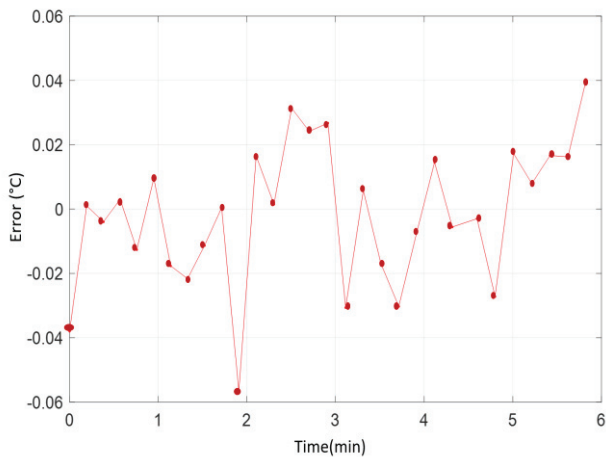


Figure 6-b. Residual errors of the temperature measurements over 10.309 m. In this example, the standard deviation on the error is equal to 0.02 °C.

Distance (m)	3.261	4.989	7.795	10.309	11.767
Offset A→B (μs)	179.5	177.3	181.2	182.7	185.6
Offset B→A (μs)	173.7	171.0	169.5	172.8	174.6

Table II. Calibration results showing the standard deviation and the optimal offset calculated from series of 30 measurements for each distance and in both directions.

A global offset can also be determined using the weighted least squares method (WLS) applied to all the distances. For each measurement of the calibration process, an offset uncertainty is assessed to define the different weights for the global offset determination.

In the uncertainty budget of the offset, the main contribution comes from the uncertainty in the speed of sound, which mainly depends on the distance measured between the measurement heads ($\sigma_d = 1$ mm) as shown in Fig 7. The other sources of uncertainty come from the environmental sensors: 3 % for the relative humidity, 1 hPa for the pressure, and 100 ppm for the CO₂ content.

In the end, global offsets of 180.5 μs is obtained for the first channel and 171.9 μs for the second. Thereafter, these values are used as the calibration values of the acoustic system.

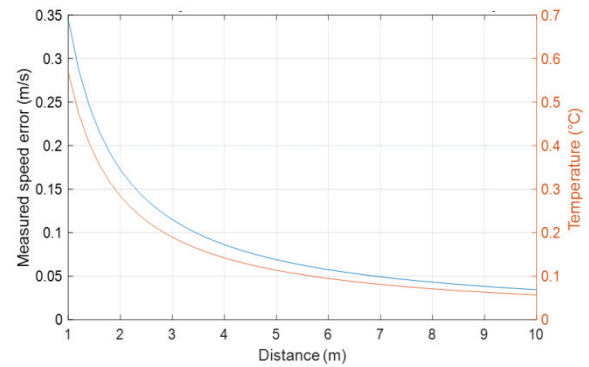


Figure 7. Speed of sound error (upper curve) and temperature measurement error (lower) induced by a 1 mm error in the distance measurements as a function of the measured distance.

5. EXPERIMENTAL VALIDATION OF THE METHOD AND SET-UP

In order to check the behavior of the developed acoustic thermometer, more specifically its linearity, measurements were performed in a room with temperature variations from 19.0 °C to 22.5 °C. The temperature of the air deduced from the acoustic thermometer was compared to the average temperature of the six Pt100 sensors set up along the pathway (cf §4.3). An example of the results is shown in Fig. 8-a and 8-b for the distance of 10.309 m, and a summary of the standard deviation of the difference between the two measurements (“Error Standard deviation”) is provided in Table III.

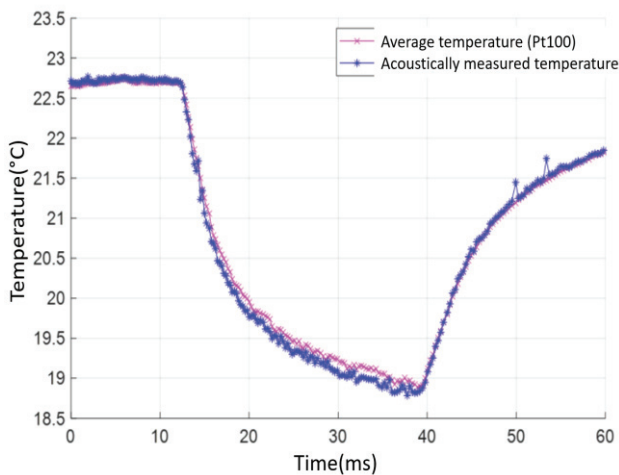


Figure 8-a. Temperature measurements over 10.309 m using the offset obtained by the calibration process.

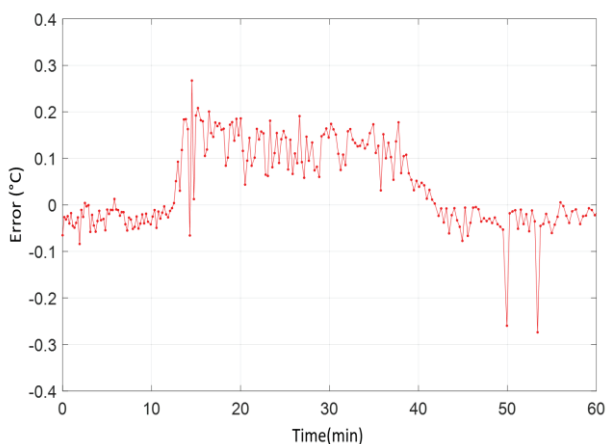


Figure 8-b. Residual errors of the temperature measurements over 10.309 m after calibration.

Distance (m)	3.261	4.989	7.795	10.309	11.767
Average error (°C)	0.06	-0.05	0.01	0.07	0.07
Error standard deviation (°C)	0.03	0.04	0.08	0.08	0.08

Table III. Temperature measurement results, values calculated from 230 measurements for each distance. The measured temperature is the average of the results obtained for both directions.

The results show a standard deviation of the error of less than 0.1 °C for measurements performed over a whole hour (230 measurement points). We remark, however, that the error is higher during the temperature fall, which is probably due to a thermalization issue on the reference temperature sensors. The real standard deviation is thus probably even smaller than that calculated from these measurements.

6. CONCLUSION

A thermometry system based on the measurement of the speed of sound has been developed. It is designed to determine the average temperature along an optical path, even in the presence of a temperature gradient, to be integrated into an absolute distance meter. It has so been designed to be compact, wireless between the two measurement heads and inexpensive. This has led to some technical choices such as an optical transmission of the signal between the acoustic transmitters and receivers, the use of a cheap and compact FPGA (Red Pitaya) for the signal generation and acquisition, and wireless communication with a computer for data processing. The validity of this experimental set-up has been checked and its performances estimated by comparison with reference temperature sensors: a standard uncertainty better than 0.1 °C has been demonstrated for distances up to 12 m. Moreover, the results show the system can track temperature variations more quickly than resistive reference temperature sensors whose speed of response is limited by thermalization issues.

7. REFERENCES

- [1] G. Bonsch and E. Potulski, ‘Measurement of the refractive index of air and comparison with modified Edlén’s formulae’, *Metrologia*, vol. 35, no. 2, pp. 133–139, Apr. 1998.
- [2] S. Robson, L. MacDonald, S. Kyle, J. Boehm, and M. Shortis, ‘Optimised multi-camera systems for dimensional control in factory environments’, *Proceedings of the Institution of Mechanical Engineers, Part B: Journal of Engineering Manufacture*, vol. 232, no. 10, pp. 1707–1718, Aug. 2018.
- [3] P. Pérez Muñoz, J. A. Albajez García, and J. Santolaria Mazo, ‘Analysis of the initial thermal stabilization and air turbulences effects on Laser Tracker measurements’, *Journal of Manufacturing Systems*, vol. 41, pp. 277–286, Oct. 2016.
- [4] J. Guillory, R. Šmíd, J. García-Márquez, D. Truong, C. Alexandre, and J.-P. Wallerand, ‘High resolution kilometric range optical telemetry in air by radio frequency phase measurement’, *Review of Scientific Instruments*, vol. 87, no. 7, p. 075105, Jul. 2016.
- [5] O. Cramer, ‘The variation of the specific heat ratio and the speed of sound in air with temperature, pressure, humidity, and CO₂ concentration’, *The Journal of the Acoustical Society of America*, vol. 93, no. 5, pp. 2510–2516, May 1993.
- [6] G. S. K. Wong, ‘Speed of sound in standard air’, *The Journal of the Acoustical Society of America*, vol. 79, no. 5, pp. 1359–1366, May 1986.
- [7] V. Korpelainen, ‘Acoustic method for determination of the effective temperature and refractive index of air in accurate length interferometry’, *Optical Engineering*, vol. 43, no. 10, p. 2400, Oct. 2004.

- [8] D. P. Massa, ‘An Overview of Electroacoustic Transducers’, p. 19
- [9] A. Hein, *Processing of SAR data*. Springer, 2003.
- [10] J. C. Jackson, R. Summan, G. I. Dobie, S. M. Whiteley, S. G. Pierce, and G. Hayward, ‘Time-of-flight measurement techniques for airborne ultrasonic ranging’, *IEEE Transactions on Ultrasonics, Ferroelectrics, and Frequency Control*, vol. 60, no. 2, pp. 343–355, Feb. 2013.
- [11] J. F. S. Costa-Júnior *et al.*, ‘Measuring uncertainty of ultrasonic longitudinal phase velocity estimation using different time-delay estimation methods based on cross-correlation: Computational simulation and experiments’, *Measurement*, vol. 122, pp. 45–56, Jul. 2018.